

Optimizing ISAC MIMO Systems with Reconfigurable Pixel Antennas

Ataher Sams¹, Yu-Cheng Hsiao², Muhammad Talha¹, Besma Smida¹, and Ashutosh Sabharwal²

¹Department of Electrical and Computer Engineering, University of Illinois Chicago, Chicago, IL, USA,

²Department of Electrical and Computer Engineering, Rice University, Houston, TX, USA

Emails: {asams3, mtalha7, smida}@uic.edu, {yh157, ashu}@rice.edu

Abstract—The integration of sensing and communication demands architectures that can flexibly exploit spatial and electromagnetic (EM) degrees of freedom (DoF). This paper proposes an Integrated Sensing and Communication (ISAC) MIMO framework that uses Reconfigurable Pixel Antenna (RPiA), which introduces additional EM-domain DoF that are electronically controlled through binary antenna coder switch networks. We introduce a beamforming architecture combining this EM and digital precoding to jointly optimize Sensing and Communication. Based on full-wave simulation of pixel antenna, we formulate a non-convex joint optimization problem to maximize sensing rate under user-specific constraints on communication rate. We utilize an Alternating Optimization framework incorporating genetic algorithm for port states of Pixel antennas, and semi-definite relaxation (SDR) for digital beamforming. Numerical results demonstrate that the proposed EM-aware design achieves considerably higher sensing rate compared to conventional arrays and enables considerable antenna reduction for equivalent ISAC performance. These findings highlight the potential of reconfigurable pixel antennas to realize efficient and scalable EM-aware ISAC systems for future 6G networks.

Index Terms—ISAC, Pixel, Reconfigurable Antenna

I. INTRODUCTION

The promise of ISAC is to re-use spectrum, hardware and waveforms to sense the environment while maintaining high communication links. To achieve this, we will require more controllable spatial Degree of Freedom (DoF) than conventional pattern-fixed arrays. An interesting solution is to move beamforming into the EM domain using reconfigurable antennas, which reshape the complex far-field pattern and the effective array manifold. This reconfigurability refers to the ability to alter properties such as frequency, radiation pattern, and polarization. Reconfigurable Pixel Antenna (RPiA)s are a canonical example, using switchable pixels to generate diverse radiation patterns. As highlighted in [1], [2], this demands physically-grounded models that capture the actual complex far-field radiation with electronically controllable switching states, rather than relying on idealized, unit-norm abstractions, to reflect real system-level trade-offs. Beyond RPiA, a few families of reconfigurable radiators have emerged

that all point to the same modeling idea: a simple “unit-norm” or “isotropic” antenna is not physically realizable, and practical “beamforming” should be EM-aware. In parasitic arrays [3], changing passive loads redistributes currents and alters both input impedance and total radiated power, so feasible beamformers are physically constrained and must be designed with the multiport circuit model in mind. In dynamic metasurface antennas (DMAs), wideband behavior (resonance, leakage, frequency selectivity) changes the set of workable precoders and can improve spectral efficiency when co-designed across EM, RF-analog, and baseband [4]. In [2], pixel-enabled electronic movable arrays use pixel coding to emulate aperture displacement without mechanics, delivering multiuser sum-rate gains with fast switching. While recent works [5], [6] formalized tri-hybrid (EM-Analog-Digital) MIMO, they relied on mathematical abstractions and focused solely on communication. These previous works also overlooked Integrated Sensing and Communication (ISAC) scenarios and the co-design of Tx/Rx/EM states with state-dependent power realization. This EM-aware reconfigurability becomes crucial for ISAC systems because, in contrast to fixed-pattern arrays, pixel antennas uniquely provide independent pattern control at each element, which is necessary to simultaneously maximize sensing gain toward radar targets and maintain communication quality to spatially separated users. We address these gaps by providing an ISAC-centric, end-to-end pattern-reconfigurable pipeline validated with actual full-wave HFSS simulations.

Our contributions are as follows- (i) Building on multiport network model, we develop an EM-aware channel model that maps binary pixel states to their true, HFSS-simulated complex far-field radiation patterns, rather than relying on idealized array responses. (ii) We pose an ISAC optimization that maximizes monostatic sensing SNR while guaranteeing per-user communication rates under transmit power and binary-state constraints at both Tx and Rx. (iii) We propose an alternating optimization (AO) solution pipeline that jointly finds the binary pixel coder states and the digital beamforming. (iv) Finally, through numerical experiments, we show that the EM-

aware, pattern-reconfigurable design significantly outperforms conventional arrays and achieves same ISAC performance with around 50% fewer antenna elements.

II. SYSTEM MODEL

Following the multiport network theory in [1], we model a RPixA as a $(Q + 1)$ -port network (see Fig. 2), including one active feeding port, denoted ‘A’, and Q pixel ports, denoted ‘P’. Its reconfigurability is enabled by a binary antenna coder $\mathbf{b} = [b_1, \dots, b_Q]^T \in \{0, 1\}^Q$, where each element b_q controls the switch on pixel port q . This coder determines the diagonal load impedance matrix $\mathbf{Z}_L(\mathbf{b}) \in \mathbb{C}^{Q \times Q}$, which is applied across Q pixel ports. We adopt the ideal switch model, where the load impedance for the q -th port is:

$$z_{L,q}(b_q) = \begin{cases} 0, & \text{if } b_q = 0 \quad (\text{switch ON}) \\ \infty, & \text{if } b_q = 1 \quad (\text{switch OFF}) \end{cases} \quad (1)$$

The current distribution of RPixA is dependent on the load impedance matrix $\mathbf{Z}_L(\mathbf{b})$. Let i_A be the feeding current and (v_A, \mathbf{v}_P) be the antenna and port voltages, respectively. We can relate the currents and voltages by

$$\begin{bmatrix} v_A \\ \mathbf{v}_P \end{bmatrix} = \begin{bmatrix} v_A \\ -\mathbf{i}_P \mathbf{Z}_L(\mathbf{b}) \end{bmatrix} = \underbrace{\begin{bmatrix} z_{AA} & \mathbf{z}_{AP} \\ \mathbf{z}_{PA} & \mathbf{Z}_{PP} \end{bmatrix}}_{\mathbf{Z}} \begin{bmatrix} i_A \\ \mathbf{i}_P(\mathbf{b}) \end{bmatrix},$$

where the impedance matrix $\mathbf{Z} \in \mathbb{C}^{(Q+1) \times (Q+1)}$ fully characterizes its radiation behavior. Thus, the full-port current vector $\mathbf{i}(\mathbf{b}) \in \mathbb{C}^{(Q+1)}$ is

$$\mathbf{i}(\mathbf{b}) = \begin{bmatrix} i_A \\ \mathbf{i}_P(\mathbf{b}) \end{bmatrix} = \begin{bmatrix} i_A \\ -(\mathbf{Z}_{PP} + \mathbf{Z}_L(\mathbf{b}))^{-1} \mathbf{z}_{PA} i_A \end{bmatrix}.$$

Similar to [1], we characterize radiation patterns by a far-field vector $\mathbf{e}_{\text{meas}}(\mathbf{b})$, which is calculated over an M -point angular grid using a fixed open-circuit radiation matrix $\mathbf{E}_{oc} \in \mathbb{C}^{M \times (Q+1)}$:

$$\mathbf{e}_{\text{meas}}(\mathbf{b}) = \mathbf{E}_{oc} \mathbf{i}(\mathbf{b}) \in \mathbb{C}^{M \times 1}. \quad (2)$$

With this complex far-field vector, which preserves both the magnitude and phase information inherent to patterns generated by a specific coder, \mathbf{b} , we can incorporate EM beamforming capabilities into our system model, as shown in Fig. 1.

A. EM-aware Beamforming Channel Architecture

In this work, we combine EM beamforming with baseband digital beamforming, leveraging the full DoF to maximize our end goal for ISAC.

EM Beamformer \mathbf{F}_{EM} : For the n -th antenna, its radiation characteristic is represented by the complex far-field vector $\mathbf{e}_n(\mathbf{b}_n)$, chosen via its coder \mathbf{b}_n . The EM

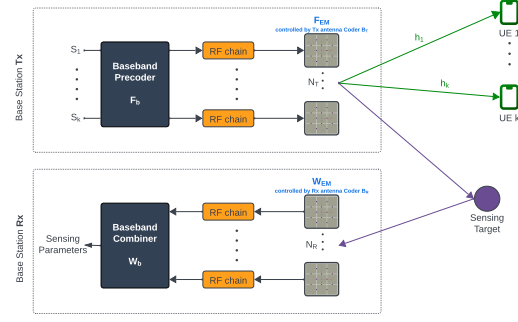


Fig. 1: Proposed EM-aware ISAC setting where a base station equipped with a RPixA performs joint MU communication and monostatic sensing.

beamformer $\mathbf{F}_{EM} \in \mathbb{C}^{M N_T \times N_T}$ is a block diagonal matrix that assembles these individual complex patterns.

$$\mathbf{F}_{EM} = \text{blkdiag}(\mathbf{e}_1(\mathbf{b}_1), \dots, \mathbf{e}_{N_T}(\mathbf{b}_{N_T})). \quad (3)$$

Digital Beamforming Architecture: We consider an ISAC system where a Base Station (BS) with N_T transmit (Tx) and N_R receive (Rx) pixel antennas senses a target and communicates with K users. The digital beamformer $\mathbf{F}_b \in \mathbb{C}^{N_T \times K}$ maps the K data streams \mathbf{s} (with $\mathbb{E}[\mathbf{s}\mathbf{s}^H] = \mathbf{I}_K$) to the antennas under a total power constraint $\|\mathbf{F}_b\|_F^2 \leq P$. The transmitted signal is

$$\mathbf{x} = \mathbf{F}_b \mathbf{s} \in \mathbb{C}^{N_T \times 1}. \quad (4)$$

To connect the digital and EM beamformers¹, we define the overall array response by the geometric steering vector $\mathbf{a}_g(\theta)$. It captures the phase progression due to the array’s physical layout, where $\mathbf{a}_g^{(t)}(\theta) \in \mathbb{C}^{N_T \times 1}$ and $\mathbf{a}_g^{(r)}(\theta) \in \mathbb{C}^{N_R \times 1}$ represent the transmit and receive steering vectors, respectively.

$$\mathbf{a}_g^{(t)}(\theta) = \frac{1}{\sqrt{N_T}} [1, e^{-j \frac{2\pi}{\lambda} d \sin \theta}, \dots, e^{-j \frac{2\pi}{\lambda} (N_T - 1) d \sin \theta}]^T.$$

With this established, we find the effective complex pattern factor, $c_n(\theta; \mathbf{b}_n)$, for the n -th antenna in direction θ by selecting the corresponding value from its complex pattern vector $\mathbf{e}_n(\mathbf{b}_n)$ using a look-angle selection vector $\mathbf{\Pi}(\theta)$ in a similar way presented in [6]:

$$c_n(\theta; \mathbf{b}_n) = \mathbf{\Pi}^T \mathbf{e}_n(\mathbf{b}_n) \in \mathbb{C}. \quad (5)$$

These complex factors are collected into diagonal matrices, $\mathbf{C}_T(\theta; \mathbf{B}_T)$ and $\mathbf{C}_R(\theta; \mathbf{B}_R)$, respectively. The final, EM-weighted array response is the element-wise product of these complex pattern factors and the geometric

¹While this model can be readily extended to include analog beamforming, we omit it here to focus on the pattern reconfigurability of RPixA. We also assume perfect self-interference mitigation, leaving the inclusion of both aspects as future work.

steering vectors. From this point forward, \mathbf{a}_T and \mathbf{a}_R will always refer to these complete, EM-weighted vectors.

$$\mathbf{a}_T(\theta; \mathbf{B}_T) = \mathbf{C}_T(\theta; \mathbf{B}_T) \mathbf{a}_g^{(t)}(\theta) \in \mathbb{C}^{N_T \times 1}, \quad (6)$$

$$\mathbf{a}_R(\theta; \mathbf{B}_R) = \mathbf{C}_R(\theta; \mathbf{B}_R) \mathbf{a}_g^{(r)}(\theta) \in \mathbb{C}^{N_R \times 1}. \quad (7)$$

B. Downlink Communication Channel

Assume each k -th user has single omnidirectional antenna. We focus on a dominant path with an angle of departure (AoD) θ_k and complex gain $\alpha_k \in \mathbb{C}$. The array-domain channel row for user k is defined as,

$$\mathbf{h}_k^H = \alpha_k \mathbf{a}_T^H(\theta_k; \mathbf{B}_T) \in \mathbb{C}^{1 \times N_T}, \quad (8)$$

where $\mathbf{a}_T(\theta_k; \mathbf{B}_T)$ is the complete EM-weighted transmit array response. The full downlink channel matrix for all K users is formed by stacking these rows: $\mathbf{H}_{dl} = [\mathbf{h}_1, \mathbf{h}_2, \dots, \mathbf{h}_K]^T \in \mathbb{C}^{K \times N_T}$. The signal received by the k -th user is-

$$y_k = \mathbf{h}_k^H \mathbf{x} + n_k = \alpha_k \mathbf{a}_T(\theta_k; \mathbf{B}_T)^H (\mathbf{F}_b \mathbf{s}) + n_k, \quad (9)$$

where $n_k \sim \mathcal{CN}(0, \sigma_k^2)$ is the AWGN noise at user k . Consequently, the per-user signal-to-interference plus noise ratio (SINR) is now defined without the analog beamforming matrix:

$$\text{SINR}_k = \frac{|\alpha_k \mathbf{a}_T(\theta_k; \mathbf{B}_T)^H \mathbf{f}_{b,k}|^2}{\sum_{j \neq k} |\alpha_k \mathbf{a}_T(\theta_k; \mathbf{B}_T)^H \mathbf{f}_{b,j}|^2 + \sigma_k^2}, \quad (10)$$

where $\mathbf{f}_{b,k}$ is the k -th column of digital beamformer \mathbf{F}_b .

III. MONOSTATIC SENSING TASK

For the sensing task, the objective of the base station (BS) is to estimate the target direction θ_s from the target reflections. The round-trip sensing channel $\mathbf{H}_s \in \mathbb{C}^{N_R \times N_T}$, which depends on both coders \mathbf{B}_T and \mathbf{B}_R , can be expressed as

$$\mathbf{H}_s(\theta_s; \mathbf{B}_T, \mathbf{B}_R) = \kappa \beta_s \mathbf{a}_R(\theta_s; \mathbf{B}_R) \mathbf{a}_T(\theta_s; \mathbf{B}_T)^H, \quad (11)$$

where $\beta_s \in \mathbb{C}$ is a complex scalar accounting for path loss and the target's radar cross-section, and $\kappa = \sqrt{N_T N_R}$ is the array scaling factor.

The transmitted signal $\mathbf{x} \in \mathbb{C}^{N_T \times 1}$ is formed by the digital beamformer $\mathbf{F}_b \in \mathbb{C}^{N_T \times K}$ as $\mathbf{x} = \mathbf{F}_b \mathbf{s}$. The echo signal is received and processed by the digital combiner $\mathbf{W}_b \in \mathbb{C}^{N_R \times N_R}$. The received baseband signal at the BS is $\mathbf{y}_s \in \mathbb{C}^{N_R \times 1}$:

$$\mathbf{y}_s = \mathbf{W}_b^H \mathbf{H}_s(\theta_s; \mathbf{B}_T, \mathbf{B}_R) \mathbf{F}_b \mathbf{s} + \tilde{\mathbf{n}}, \quad (12)$$

where $\tilde{\mathbf{n}} \in \mathbb{C}^{N_R \times 1}$ represents the receiver noise. The quality of the sensing is determined by the Sensing signal to noise ratio (SNR) of this processed echo, which we denote as:

$$\gamma_{\text{rad}} = \frac{|\beta_s|^2 \kappa^2}{\sigma_n^2} \|\mathbf{a}_T(\theta_s; \mathbf{B}_T)^H \mathbf{F}_b\|_F^2 \|\mathbf{W}_b^H \mathbf{a}_R(\theta_s; \mathbf{B}_R)\|_F^2 \quad (13)$$

A. Comparison with conventional antenna array

To compare the performance of a pixel antenna array with a conventional antenna array, we look at the norm of the channel matrices of both cases. For the pixel antenna structure, the effective norm of the array response matrix can be given as

$$\begin{aligned} \|\mathbf{H}_s(\theta_s; \mathbf{B}_T, \mathbf{B}_R)\|_F^2 &= \|\mathbf{a}_R(\theta_s; \mathbf{B}_R)\|^2 \|\mathbf{a}_T(\theta_s; \mathbf{B}_T)\|^2 \\ &= \frac{1}{N_T N_R} \left(\sum_{n=1}^{N_T} |c_n^T(\theta_s; \mathbf{b}_n^T)|^2 \right) \left(\sum_{n=1}^{N_R} |c_n^R(\theta_s; \mathbf{b}_n^R)|^2 \right). \end{aligned} \quad (14)$$

For the conventional case, we can write the array response matrix norm as $\|\mathbf{a}_R(\theta) \mathbf{a}_T^H(\theta)\|_F^2 = \|\mathbf{a}_R(\theta)\|^2 \|\mathbf{a}_T(\theta)\|^2 = 1$. For pixel antenna we can decouple the transmitter and receiver side to get

$$\begin{aligned} \min_{i \in \{T, R\}} \|\mathbf{a}_i(\theta_s; \mathbf{B}_i)\|^2 &\geq 1 \\ \|\mathbf{a}_i(\theta_s; \mathbf{B}_i)\|^2 &\geq 1, \quad \forall i \in \{T, R\}. \end{aligned} \quad (15)$$

In (15), we have effectively decoupled the transmitter (TX) and receiver (RX) sides and hence we can look at them individually as $\|\mathbf{a}_i(\theta; \mathbf{B}_i)\|^2 = \frac{1}{N_i} \sum_{k=1}^{N_i} |c_k^i(\theta; \mathbf{b}_k^i)|^2$. If we want to have more gain than the conventional antenna array, then the following condition needs to be satisfied

$$\sum_k |c_k^i(\theta; \mathbf{b}_k^i)|^2 \geq N_i, \quad i \in \{T, R\}. \quad (16)$$

In other words, the collective gain of all the antennas towards the target direction should be greater than the conventional antenna. In order to further expand the (16), we consider two strategies to normalize the radiated power of each antenna in order to make a fair comparison against an isotropic conventional antenna: (1) total radiated power (TRP) normalization and (2) port current normalization, which we will explain shortly. For TRP normalization we write (16) as

$$\sum_k |c_k^i(\theta; \mathbf{b}_k^i)|^2 = \sum_k \left| \frac{\mathbf{\Pi}^T(\theta) \mathbf{e}_{\text{meas}}(\mathbf{b}_k^i)}{\|\mathbf{e}_{\text{meas}}(\mathbf{b}_k^i)\|_2} \right|^2 \geq \frac{N_i}{M}, \quad (17)$$

where, for our 2D azimuthal pattern at fixed elevation, this discrete approximation of TRP is defined as $\text{TRP}(\mathbf{b}) = \frac{1}{M} \sum_{m=1}^M |\mathbf{e}_{\text{meas},m}(\mathbf{b})|^2$, where $\mathbf{e}_{\text{meas},m}(\mathbf{b})$ is the complex field at the m -th sampled angle $\theta_m \in [\theta_{\min}, \theta_{\max}]$ calculated through Equ. (2). This ensures $\frac{1}{M} \sum_{m=1}^M |\mathbf{e}_m(\mathbf{b})|^2 = 1$ for all coder states \mathbf{b} , equivalently $\|\mathbf{e}(\mathbf{b})\|_2^2 = M$. For comparison, a conventional isotropic element with uniform angular response satisfies the same unit TRP condition after normalization, establishing a fair performance baseline.

For the current norm, we normalize the $\mathbf{e}_{\text{meas}}(\mathbf{b})$ with the norm of the input current to the ports, i.e.,

$\mathbf{i}(\mathbf{b})$ as $\mathbf{e}(\mathbf{b}) = \frac{\mathbf{e}_{\text{meas}}(\mathbf{b})}{\|\mathbf{i}(\mathbf{b})\|}$. The rationale behind this is that we normalize the input power to the antenna ports. By using the current norm, the required threshold for better performance for $i \in \{T, R\}$, as compared to a conventional antenna, becomes,

$$\sum_k |c_k^i(\theta, \mathbf{b}_k^i)|^2 = \sum_k \left| \frac{\mathbf{\Pi}^T(\theta) \mathbf{e}_{\text{meas}}(\mathbf{b}_k^i)}{\|\mathbf{i}(\mathbf{b}_k^i)\|_2} \right|^2 \geq N_i. \quad (18)$$

IV. OPTIMIZATION PROBLEM AND SOLUTION

The objective of our work is to design our beamforming matrices as well as pixel antenna switch states such that the sensing performance is maximized subject to given data rate constraints. In particular, from (13), that the radar SNR given as

$$\hat{\gamma}_{\text{rad}} = \frac{\left\| \mathbf{W}_b^H \hat{\mathbf{H}}_s(\theta_s; \mathbf{B}_T, \mathbf{B}_R) \mathbf{F}_b \right\|_F^2}{\sigma_b^2}, \quad (19)$$

where $\hat{\mathbf{H}}_s = \mathbf{a}_R(\theta; \mathbf{B}_R) \mathbf{a}_T^H(\theta; \mathbf{B}_T)$. With the help of (19), the optimization problem we aim to solve is

$$\max_{\mathbf{W}_b, \mathbf{F}_b, \mathbf{B}_R, \mathbf{B}_T} \hat{\gamma}_{\text{rad}} \quad (20a)$$

$$\text{s.t. } \text{SINR}_k \geq r_k, \quad \forall k \in \mathcal{K} \quad (20b)$$

$$\|\mathbf{W}_b\|_F^2 \leq 1, \quad (20c)$$

$$\|\mathbf{F}_b\|_F^2 \leq P, \quad (20d)$$

$$\mathbf{b}_i^T \in \{0, 1\}^Q, \quad \forall i \in \{1, \dots, N_t\} \quad (20e)$$

$$\mathbf{b}_i^R \in \{0, 1\}^Q, \quad \forall i \in \{1, \dots, N_r\} \quad (20f)$$

$$\sum_{k=1}^{N_i} |c_k^i(\theta, \mathbf{b}_k^i)|^2 \geq N_i \quad \forall i \in \{T, R\}. \quad (20g)$$

where (20a) is radar SNR maximization objective function, (20b) is the per user SINR constraint, (20e) and (20f) are the pixel antenna switches state constraints.

To find the solution of (20), we employ the strategy of AO and solve this by only assuming one variable active (others constant) at a time. We start with the optimization of \mathbf{B}_T and \mathbf{B}_R and then move towards the digital beamforming optimization².

A. Optimization of \mathbf{B}_T and \mathbf{B}_R

To solve for both \mathbf{B}_T and \mathbf{B}_R given digital beamformings, we note that both the objective function and users' SINR constraints are highly nonlinear in \mathbf{B}_T and \mathbf{B}_R due to constraints (20e) and (20f). Hence, we rely on the genetic algorithm (GA) [7] to find the optimal \mathbf{B}_T and \mathbf{B}_R . We want to emphasize that GA has been extensively utilized in pixel antenna design systems [8], [9]. We use

²The reason for choosing this strategy is that it can reduce the number of AO iterations required to reach the solution. For instance, if we start with the optimization of \mathbf{F}_b or \mathbf{W}_b for a given random \mathbf{H}_s , it might be possible that the given \mathbf{B}_T and \mathbf{B}_R make the vector $\mathbf{C}_T(\theta_s; \mathbf{B}_T) \mathbf{a}_T^H(\theta_s)$ orthogonal to optimal \mathbf{F}_b or \mathbf{W}_b , which may in return require more number of AO iterations.

the Lagrangian relaxation to incorporate users' channel strength in the objective function as follows

$$\max_{\mathbf{B}_T, \mathbf{B}_R} \left\| \hat{\mathbf{H}}_s(\theta_s; \mathbf{B}_T, \mathbf{B}_R) \right\|_F^2 + \sum_k \lambda_k \|\mathbf{a}_T(\phi_k; \mathbf{B}_T)\|^2 \quad (21)$$

Expanding the norm of the sensing channel, we can get $\|\hat{\mathbf{H}}_s(\theta_s; \mathbf{B}_T, \mathbf{B}_R)\|_F^2 = \|\mathbf{a}_R(\theta; \mathbf{B}_R)\|^2 \|\mathbf{a}_T(\theta; \mathbf{B}_T)\|^2$.

As the user channel gain is independent of \mathbf{B}_R , we can have two parallel GA problems which we solve numerically,

$$\mathcal{G}_1 : \max_{\mathbf{B}_T} \|\mathbf{a}_T(\theta; \mathbf{B}_T)\|^2 + \sum_{k \in \mathcal{K}} \lambda_k \|\mathbf{a}_T(\phi_k; \mathbf{B}_T)\|^2 \quad (22a)$$

$$\text{s.t. (20e), (20g).}$$

$$\mathcal{G}_2 : \max_{\mathbf{B}_R} \|\mathbf{a}_R(\theta; \mathbf{B}_R)\|^2 \quad (22b)$$

$$\text{s.t. (20f), (20g).}$$

B. Optimization of \mathbf{F}_b and \mathbf{W}_b

To optimize (20) for a given \mathbf{B}_T and \mathbf{B}_R , since \mathbf{W}_b affects only the sensing SNR, it is chosen as the left singular vectors of $\hat{\mathbf{H}}_s(\theta_s)$, i.e., $\mathbf{W}_b^* = \mathbf{U}_{\hat{\mathbf{H}}_s}$, where $\mathbf{U}_{\hat{\mathbf{H}}_s}$ are the left singular vectors of $\hat{\mathbf{H}}_s(\theta_s)$.

For finding the optimal \mathbf{F}_b , we employ the Semi-definite relaxation (SDR) method by relaxing the problem by using SDR of rank one matrices $\mathbf{F}_{b,k} = \mathbf{f}_{b,k} \mathbf{f}_{b,k}^H$. The objective function can then be written as

$$\max_{\mathbf{F}_{b,k} \forall k \in \mathcal{K}} \text{Tr}(\hat{\mathbf{H}}_s(\theta_s)^H \hat{\mathbf{H}}_s(\theta_s) \sum_k \mathbf{F}_{b,k}) \quad (23)$$

The objective function is now linear in each $\mathbf{F}_{b,k}$. The SINR constraints for a user k can be written as

$$\frac{|\alpha_k|^2}{r_k} \text{Tr}(\mathbf{A}_k(\phi_k) \mathbf{F}_{b,k}) \geq \sum_{j \neq k} (|\alpha_k|^2 \text{Tr}(\mathbf{A}_k(\phi_k) \mathbf{F}_{b,j})) + \sigma_k^2, \quad (24)$$

where $\mathbf{A}_k(\phi_k, \mathbf{B}_T) = \mathbf{a}_T(\phi_k) \mathbf{a}_T^H(\phi_k)$. Using this relaxation, we need rank-one solutions, which will introduce nonconvexity in the problem. Relaxing the rank-one constraint, the problem becomes

$$\max_{\mathbf{F}_{b,k} \forall k \in \mathcal{K}} \text{Tr} \left(\hat{\mathbf{H}}_s^H(\theta_s) \hat{\mathbf{H}}_s(\theta_s) \sum_k \mathbf{F}_{b,k} \right) \quad (25)$$

$$\text{s.t. } \text{Tr} \left(\sum_k \mathbf{F}_{b,k} \right) \leq P, \quad \text{and } (24).$$

The relaxed problem (25) may not be tight; the optimal solution of (25) can give us solutions with more than rank-one. However, following the strategy defined in [10], we can get the rank-one optimal solutions, from which we can construct the optimal \mathbf{F}_b^* . We summarize the overall optimization framework in Algorithm 1.

Algorithm 1 Pixel and beamforming optimization

Input: $\theta, \phi_1, \phi_2, \dots, \phi_K, I$
Output: $\mathbf{B}_T, \mathbf{B}_R, \mathbf{W}_b, \mathbf{F}_b$

- 1: $i \leftarrow 1$
 - 2: \mathbf{B}_T and $\mathbf{B}_R \leftarrow$ solve (22)
 - 3: $\mathbf{W}_b \leftarrow \frac{\mathbf{U}_{\text{Hrad}}}{\|\mathbf{U}_{\text{Hrad}}\|_F}$
 - 4: $\{\mathbf{F}_{b,k} \forall k \in \mathcal{K}\} \leftarrow$ solve (25)
 - 5: **for** $k \in \mathcal{K}$ **do**
 - 6: **if** $\text{rank}(\mathbf{F}_{b,k}) \neq 1$ **then**
 - 7: $\mathbf{f}_{b,k} \leftarrow (\mathbf{h}_k^H \mathbf{F}_{b,k} \mathbf{h}_k)^{-1/2} \mathbf{F}_{b,k} \mathbf{h}_k$
 - 8: **else**
 - 9: $\mathbf{F}_{b,k} = \lambda_k \mathbf{q}_k \mathbf{q}_k^H$ and $\mathbf{f}_{b,k} \leftarrow \lambda_k \mathbf{q}_k$
 - 10: **end if**
 - 11: **end for**
-

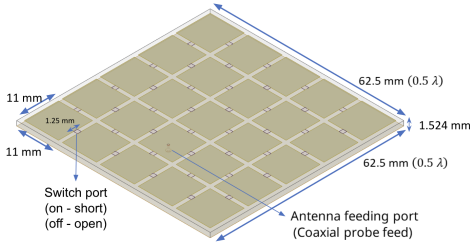


Fig. 2: Geometry of proposed pixel antenna featuring one coaxial feeding port and $Q = 40$ pixel ports

V. NUMERICAL RESULTS

Reconfigurable Pixel Antenna Design. We present a 5×5 pixel antenna for 2.4 GHz in Fig. 2 with pattern reconfigurability via electronically controlled switches. The dimension of aperture is $0.5\lambda \times 0.5\lambda$ ($\lambda = 125$ mm), includes metallic pixels (11 mm \times 11 mm) separated by 1.25 mm gaps. The Rogers RO4003 is selected for the substrate due to its low dielectric loss. There are 40 RF switches (2^{40} possible states) between pixels encoded by a binary coder $\mathbf{b} \in \{0, 1\}^{40}$. Excitation is provided by a coaxial probe optimized for 50 Ω impedance matching. Fig. 3 illustrates pattern reconfigurability of a RPixA for five random binary coder states under the two normalization approaches. This highlights the benefit of goal-oriented reconfigurable pattern selection and ensures a fair comparison with isotropic antennas.

Simulation Setup and Parameters. The simulation framework is implemented in MATLAB, utilizing full-wave electromagnetic data from HFSS 2025 R1. Key system parameters include a 2.4 GHz carrier frequency (f_c) with $\lambda/2$ element spacing (62.5 mm), a total transmit power (P_{total}) of 20 dBW, and a uniform noise power of -80 dBm for both users and sensing. The target distance is 40 m, with $\text{PathLoss}(d) = \text{FSPL} +$

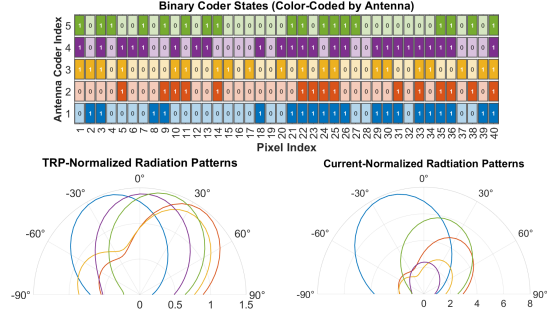


Fig. 3: Radiation patterns for five random Antenna coder of one single RPixA; (a) Binary coder states, where light color denotes 0 \rightarrow switch on, and dark color denotes 1 \rightarrow switch off (b) TRP-normalized patterns; (c) current-normalized patterns. Colors are consistent across all panels.

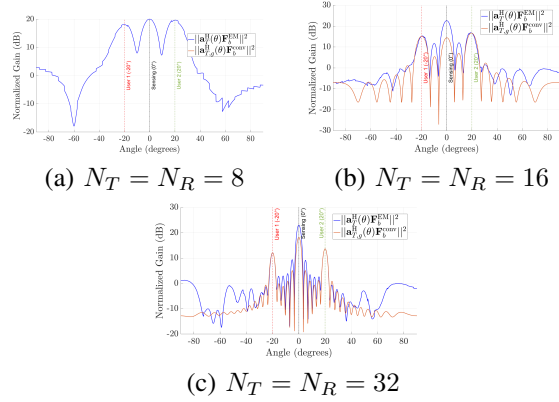


Fig. 4: Optimized Tx beampatterns for different array sizes. Blue: EM-optimized ($|\mathbf{a}_T^H(\theta) \mathbf{F}_b^{\text{EM}}|^2$); red: conventional ($|\mathbf{a}_{T,g}^H(\theta) \mathbf{F}_b^{\text{conv}}|^2$). Dashed lines denote User 1 (-20°), sensing target (0°), and User 2 (20°).

$10n \log_{10}(d) + \sigma$ (where $n = 2$ and $\sigma = 2.9$ dB). For the Genetic Algorithm, a population size of 300 and a maximum of 200 generations are used.

Beampattern Analysis. Fig. 4 compares the optimized Tx beampatterns for 8, 16, and 32-element arrays using our EM-aware RPixA model against a conventional isotropic model. With a sensing target at 0° , users at $[-20^\circ, 20^\circ]$, the EM-optimized design consistently achieves higher peak gain with three distinct main lobes. The conventional design fails to find a feasible solution for $N = N_T = N_R = 8$. The EM-aware design shows a 29% higher sensing rate for $N = 16$ (17.85 vs. 13.8 bps/Hz) and a 17% improvement for $N = 32$ (19.93 vs. 17.06 bps/Hz), all while satisfying communication rate of 10 bps/Hz.

Sensing Rate and Efficiency Analysis. Fig. 5a evaluates sensing rate versus user rate requirements (1–14 bps/Hz) for a 32-element array with users at $[-20^\circ, 20^\circ]$

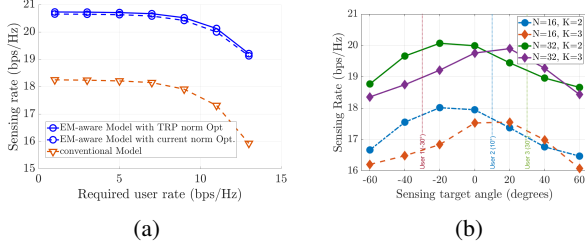


Fig. 5: Performance comparison of sensing rates with (a) varying user SINR and (b) varying target angle.

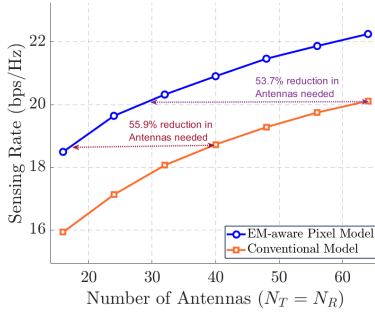


Fig. 6: Sensing rate vs array size comparison between EM-aware pixel model and conventional model for user rate constraint of 8 bps/Hz.

and a target at 0° . Both EM-aware normalization methods (TRP and port current) are nearly identical and consistently outperform the conventional model; so only the TRP-normalized results are used in the subsequent plots. The sensing rate is stable for low user rates ($R_k < 8$ bps/Hz) but degrades at higher constraints, as the optimization must allocate more power to meet the exponential communication SINR requirement ($r_k = 2^{R_k} - 1$), confirming the fundamental ISAC trade-off. Subsequently, Fig. 5b illustrates sensing rate versus target angle for $N = 16$ and $N = 32$ arrays. For two users ($K = 2$, at $[-30^\circ, 10^\circ]$), peak rates occur near -20° (20.1 bps/Hz for $N = 32$, 18.0 bps/Hz for $N = 16$). For three users ($K = 3$, at $[-30^\circ, 10^\circ, 30^\circ]$), peaks are near 20° (19.8 bps/Hz for $N = 32$, 17.6 bps/Hz for $N = 16$). This confirms that maintaining high sensing rates is more difficult when the sensing targets are far from the users.

Leveraging EM-aware beamforming reduces the required RF chains and antennas for equivalent performance. Figure 6 demonstrates this by plotting sensing rate versus array size for a two-user scenario (8 bps/Hz rate constraint). The EM-aware pixel model consistently outperforms the conventional design, achieving an average sensing rate improvement of 2.28 bps/Hz. Significantly, the EM-optimized approach enables substantial hardware reduction. For example, only 30 pixel

antennas are required to match the 20.12 bps/Hz sensing rate of a conventional 64-element array, representing a 53.7% reduction in number of antenna and RF-chains. This antenna reduction directly lowers cost and power consumption while maintaining identical ISAC performance, demonstrating the scalability and robustness of the reconfigurable pixel antenna approach.

VI. CONCLUSION

We presented an EM-aware optimization framework for ISAC utilizing RPixA. By bridging full-wave EM simulation with digital precoder design, we unlock new DoF that were previously unattainable in a conventional fixed pattern antenna array. Through binary antenna coders and a joint optimization pipeline, the work demonstrates how EM-level reconfigurability enhances ISAC performance. Future work will focus on developing faster and more efficient optimization algorithms, reducing the pixel-state search space, and incorporating reflection coefficient and coupling effects for more accurate EM modeling. Additionally, extending the framework to multi-band and polarization-reconfigurable designs will introduce a new frontier for 6G.

REFERENCES

- [1] S. Shen, K.-K. Wong, and R. Murch, "Antenna Coding Empowered by Pixel Antennas," *IEEE Transactions on Communications*, 2025.
- [2] K. Chen, C. Qi, Y. Hong, and C. Yuen, "REMAA: Reconfigurable Pixel Antenna-based Electronic Movable-Antenna Arrays for Multiuser Communications," *IEEE Transactions on Communications*, 2025.
- [3] N. V. Deshpande, M. R. Castellanos, S. R. Khosravirad, J. Du, H. Viswanathan, and R. W. Heath Jr, "Beamforming with hybrid reconfigurable parasitic antenna arrays," *arXiv preprint arXiv:2502.17864*, 2025.
- [4] J. Carlson, N. V. Deshpande, M. R. Castellanos, and R. W. Heath, "A Wideband Beamforming Algorithm for Dynamic Metasurface Antennas under Realistic Constraints," in *IEEE International Conference on Communications*, pp. 3922–3927, IEEE, 2025.
- [5] P. Zheng, Y. Zhang, T. Y. Al-Naffouri, M. J. Hossain, and A. Chaaban, "Tri-Hybrid Multi-User Precoding Using Pattern-Reconfigurable Antennas: Fundamental Models and Practical Algorithms," *arXiv preprint arXiv:2505.08938*, 2025.
- [6] M. Liu, M. Li, R. Liu, and Q. Liu, "Tri-timescale Beamforming Design for Tri-hybrid Architectures with Reconfigurable Antennas," *arXiv preprint arXiv:2503.03620*, 2025.
- [7] D. S. Weile and E. Michielssen, "Genetic Algorithm Optimization Applied to Electromagnetics: A Review," *IEEE Transactions on Antennas and Propagation*, vol. 45, no. 3, pp. 343–353, 1997.
- [8] S. Song and R. D. Murch, "An Efficient Approach for Optimizing Frequency Reconfigurable Pixel Antennas Using Genetic Algorithms," *IEEE Transactions on Antennas and Propagation*, vol. 62, no. 2, pp. 609–620, 2014.
- [9] S. Soltani, P. Lotfi, and R. D. Murch, "Design and Optimization of Multipoint Pixel Antennas," *IEEE Transactions on Antennas and Propagation*, vol. 66, no. 4, pp. 2049–2054, 2018.
- [10] H. Hua, J. Xu, and T. X. Han, "Optimal Transmit Beamforming for Integrated Sensing and Communication," *IEEE Transactions on Vehicular Technology*, vol. 72, no. 8, pp. 10588–10603, 2023.